Anesthesiology 2001; 95:1406–1413

Ketamine Blockade of Voltage-gated Sodium Channels

Evidence for a Shared Receptor Site with Local Anesthetics

Larry E. Wagner II, B.S., Kevin J. Gingrich, M.D.,† John C. Kulli, M.D.,‡ Jay Yang, Ph.D., M.D.§*

Background: **The general anesthetic ketamine is known to be an *N*-methyl-D-aspartate receptor blocker. Although ketamine also blocks voltage-gated sodium channels in a local anesthetic–like fashion, little information exists on the molecular pharmacology of this interaction. We measured the effects of ketamine on sodium channels.**

Methods: **Wild-type and mutant (F1579A) recombinant rat skeletal muscle sodium channels were expressed in *Xenopus* oocytes. The F1579A amino acid substitution site is part of the intrapore local anesthetic receptor. The effect of ketamine was measured in oocytes expressing wild-type or mutant sodium channels using two-electrode voltage clamp.**

Results: **Ketamine blocked sodium channels in a local anesthetic–like fashion, exhibiting tonic blockade (concentration for half-maximal inhibition [IC_{50}] = 0.8 mM), phasic blockade (IC_{50} = 2.3 mM), and leftward shift of the steady-state inactivation; the parameters of these actions were strongly modified by alteration of the intrapore local anesthetic binding site (IC_{50} = 2.1 mM and IC_{50} = 10.3 mM for tonic and phasic blockade, respectively). Compared with lidocaine, ketamine showed greater tonic inhibition but less phasic blockade.**

Conclusions: **Ketamine interacts with sodium channels in a local anesthetic–like fashion, including sharing a binding site with commonly used clinical local anesthetics.**

KETAMINE, an arylcyclohexylamine-derived intravenous general anesthetic, also has well-documented local anesthetic–like action. Experimentally, ketamine blocks sodium-dependent action potentials in dorsal root ganglion neurons,[1] cardiac myocytes,[2] and frog myelinated nerve fibers.[3] Clinically, neuraxial administration of ketamine *via* the intrathecal or the epidural route has been used in veterinary and human patients.[4–7] Despite abundant phenomenologic reports that ketamine possesses local anesthetic–like properties, the exact mechanism of the interaction between ketamine and voltage-gated sodium channels is unknown.

Unambiguous classification of a drug as a local anesthetic requires it to demonstrate a concentration-dependent reduction of sodium channel current and a leftward shift in the steady-state inactivation curve; both of these effects must involve an intrapore local anesthetic binding site.[8,9] Mechanistic studies of ketamine's actions on sodium channels are few and conflicting. Hara *et al.*[2] reported the predominant effect of ketamine to be tonic inhibition, with little use-dependent, or phasic, blockade. In contrast, Zhou and Zhao[1] found both tonic and phasic ketamine block in dorsal root ganglion neurons. Benoit[3] reported no effect of ketamine on the sodium channel steady-state inactivation curve, but other investigators[1,10] found a shift in the hyperpolarized direction, a characteristic of local anesthetics.

Because of the conflicting reports and the lack of a quantitative description of ketamine blockade, we investigated the local anesthetic–like action of ketamine in recombinantly expressed rat skeletal muscle ($rSkM_1$) voltage-gated sodium channels. We also directly investigated the ketamine anesthetic binding site through expression of a mutant channel. The $rSkM_1$ F1579A mutation alters the binding properties of the critical residue on domain IV, transmembrane segment 6 (IVS6), which constitutes part of the intrapore local anesthetic receptor.[11]

Materials and Methods

Molecular Biology

The α-subunit and the accessory β_1 subunit of the rat skeletal muscle μ_1 sodium channel were inserted in a modified pBluescript (KS−) at the EcoR I site. Sodium channel expression in oocytes requires coinjection with β_1 to duplicate *in vivo* channel function. *Xenopus* β-globin–untranslated regions flanked the multiple cloning site in the vector to enhance stability of the transcribed complementary RNA (cRNA). Recombinantly expressed rat skeletal muscle ($rSkM_1$) was mutated from wild-type to the F1579A mutant using sequential polymerase chain reaction–based mutagenesis. Presence of the intended mutation and the lack of spurious errors were confirmed by automatic sequencing. DNA was transcribed to cRNA using the Message Machine T3 transcription kit (Ambion Inc., Austin, TX).

Oocyte Expression

Xenopus oocytes were obtained from frogs purchased from Nasco (Fort Atkinson, WI). In preparation for cRNA injection and electrical recording, oocytes were defolliculated by exposure to 0.2 mg/ml collagenase (type IA; Sigma Chemical Company, St. Louis, MO) for 1–3 h

* Technical Associate II, ‡ Professor of Anesthesiology, Department of Anesthesiology, § Associate Professor of Anesthesiology, Pharmacology and Physiology. † Associate Professor, Department of Anesthesiology. Current position: Department of Anesthesia, Northwestern Medical Center, St. Albans, Vermont.

Received from the Department of Anesthesiology, University of Rochester Medical Center, Rochester, New York. Submitted for publication March 26, 2001. Accepted for publication July 18, 2001. Supported by grant No. BC971561 from the US Army Medical Research and Materiel Command, Fort Detrick, Maryland; grant No. RO1 GM52325 from the National Institutes of Health, Bethesda, Maryland; and the Department of Anesthesiology, University of Rochester Medical Center, Rochester, New York. Presented in part at the meeting of the Biophysical Society, Boston, Massachusetts, February 19, 2001.

Address reprint requests to Dr. Yang: Box 604, Department of Anesthesiology, University of Rochester Medical Center, 601 Elmwood Avenue, Rochester, New York 14642. Address electronic mail to: jay_yang@urmc.rochester.edu. Individual reprint requests may be purchased through the Journal web site, www.anesthesiology.org.

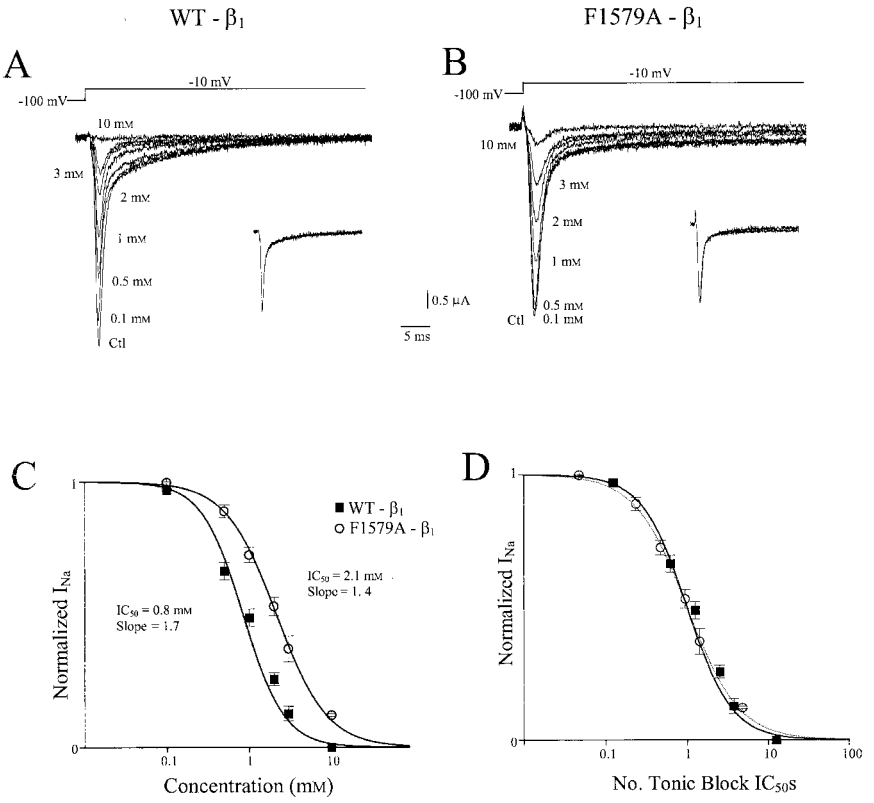

Fig. 1. Tonic Block by Ketamine. Na^+ currents (I_{Na}) recorded from oocytes expressing WT-β_1 (*A*) and F1579A-β_1 (*B*), elicited by a step depolarization from −100 to −10 mV in the presence of increasing concentrations of ketamine. (*A, inset*) and (*B, inset*) Insets in *A* and *B* are current traces normalized to control (no ketamine) for WT-β_1 in 1 mM ketamine and F1579A-β_1 in 2 mM ketamine, respectively. The normalized trace for WT-β_1 perfectly superimposes the control response, indicating that ketamine does not alter current kinetics. (*C*) Normalized grouped data (n = 5–9): concentration–response relation of ketamine for WT-β_1 and F1579A-β_1. (*D*) Replot of the grouped data *versus* concentration in units of IC_{50}. The solid lines are the logistic fits with indicated parameters.

at room temperature. Oocytes were injected with 50 nl (5 ng) of 5' capped cRNA of α_{WT} or α_{F1579A} with β_1 (1:1 ratio by mass), referred to as WT-β_1 and F1579A-β_1, respectively. The oocytes were incubated for 1 or 2 days at 16°C and tested for expression using the two-electrode voltage clamp technique.

Two-electrode Oocyte Voltage Clamp

Bath solution contained 100 mM NaCl, 2 mM KCl, 1.8 mM $CaCl_2$, 1 mM $MgCl_2$, and 5 mM HEPES; pH was adjusted to 7.6 with NaOH at 22°C. Oocyte currents were examined using a standard two-microelectrode voltage clamp technique. Electrodes were pulled from borosilicate glass pipettes and filled with 3 M KCl. Electrode resistances were 0.2–0.6 MΩ. Transmembrane potential was controlled with a voltage clamp amplifier (Model OC-725C; Warner Instruments, Hamden, CT). Only currents greater than 10 μA were analyzed to minimize clamp error. A grounded metal shield was inserted between the two electrodes to minimize electrode coupling and to speed clamp rise time. Typical charging curves were approximated by monoexponential functions with time constants less than 0.3 ms.

Voltage commands were generated by a 12-bit digital/analog converter driven by software of our own design written in Axobasic (Axon Instruments, Foster City, CA). Currents were filtered at 1 kHz (−3 dB, four-pole Bessel) and sampled at greater than 4 kHz by a 12-bit analog/digital converter. Capacity transients were compensated for using a pulse train protocol in which P/6 pulses were applied at least 10 s before data collection to prevent artifact.

Cells were held at −100 mV between infrequent test pulses (−10 mV, 20 ms, minimal interval of 10 s). This protocol allowed inactivated channels to return to the resting state between pulses. Cells exposed to 0–10 mM ketamine required approximately 5 min for Na^+ current magnitudes to stabilize. All currents returned to control value after washout of drug solutions indicating full reversibility of the drug effects.

Statistical and Data Analysis

Normalized current concentration–response relations were fitted with the following logistic equation

$$I = 1/(1 + (C/IC_{50})^{Slope}) \quad (1)$$

where I is current magnitude normalized by control, C is the agent concentration, IC_{50} is the half-blocking concentration, and Slope is a slope factor related to the Hill coefficient. Normalized current amplitude responses over time were fitted with a multiexponential function

$$I = \Sigma A_i \exp(-t/\tau_i) \quad (2)$$

where I is the normalized current, t is time, Ai represents the component amplitudes, and τ_i is the time constant of the ith exponential component. Normalized current voltage response relations were fit with the two-state Boltzmann equation

$$I = 1/(1 + \exp[(V - V_{½})/slope_b]) \quad (3)$$

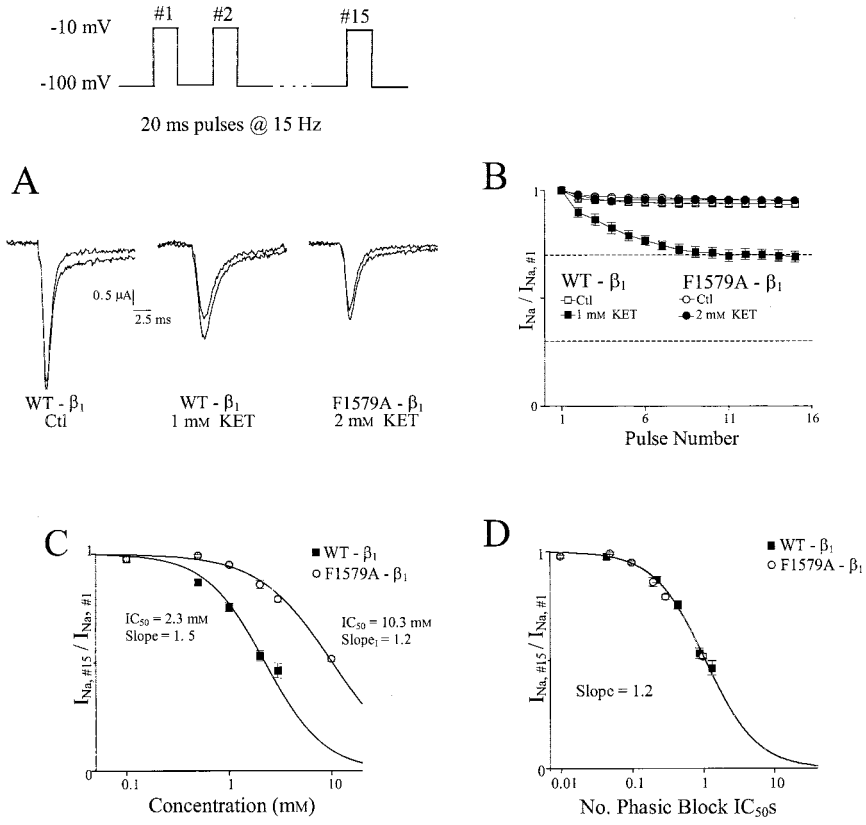

Fig. 2. Use-dependent phasic blockade. Use-dependent (or phasic) blockade was assayed using a 15-Hz pulse train protocol (*top*). (*A*) Representative current traces (pulses 1 and 15) for WT-β_1 control, WT-β_1 in 1 mM ketamine, and F1579A-β_1 in 2 mM ketamine. (*B*) Plot of Na^+ current (I_{Na}) amplitudes for each pulse normalized to that of pulse 1 *versus* pulse number for WT-β_1 control (n = 11); 1 mM ketamine (n = 6); F1579A-β_1 control (n = 11); and 2 mM ketamine (n = 5). Dashed lines represent plateau values of the responses for WT-β_1 in 1 mM ketamine and 2 mM lidocaine. These concentrations of ketamine are equipotent. (*C*) Plot of the ratio of peak I_{Na} of pulse 15 to pulse 1 *versus* ketamine concentration (n = 3–6). Solid lines are the logistic fits with indicated parameters. (*D*) Replots of the grouped data *versus* concentration in units of IC_{50}.

where I is the current amplitude normalized by control, V is membrane voltage, $V_{½}$ is the voltage at half value, and $slope_b$ is a slope factor. Equation parameters were estimated using a nonlinear, least-squares algorithm. Two-tailed *t* tests with *P* values < 0.05 were considered to have statistical significance.

Three-dimensional Molecular Modeling

Three-dimensional chemical structures for ketamine were modeled using HyperChem (Hypercube, Inc., Waterloo, Ontario, Canada). The optimum geometry of the molecule in an aqueous environment was determined by energy minimization of a periodic box (18.7-Å cube) filled with water molecules and a molecule of ketamine. The energy minimization was accomplished by the Polak-Ribiere algorithm using the MM+ force field,[12] and the resulting energetically optimum molecular conformation was rotated in space to visually determine the size of the molecule in the three spatial axes. The calculated dimensions were as follows: X = the minimum width dimension, Y = the intermediate width dimension, and Z = the maximum length dimension. XY determines the minimal end-on cross-sectional area thought to be a critical determinant of drug access to the channel inner vestibule through the hydrophobic pathway.[13] We carried out the same modeling technique on several local anesthetic molecules and arrived at dimensions comparable to those previously reported by Courtney,[13] confirming the validity of this molecular modeling technique.

Results

We first explored ketamine blockade of resting channels. Figures 1A and B show families of sodium currents (I_{Na}) evoked from oocytes expressing either WT-β_1 or the mutation F1579A-β_1 in the presence of a range of ketamine concentrations. In WT-β_1 (fig. 1A), control I_{Na} evoked upon depolarization to −10 mV in the absence of ketamine displays a typical current time course, peaking within a few milliseconds (downward deflection represents inward current flow through the open channels). The current then decayed, reflecting rapid channel closing or inactivation. Ketamine applied before membrane depolarization depressed WT-β_1 peak current in a concentration-dependent fashion, reflecting blocked channels. There was no change in current time course; after normalization, control and 1-mM ketamine responses overlapped (fig. 1A). This result argues for blockade of closed resting channels. Similarly, ketamine depressed F1579A-β_1 peak current (fig. 1B) in a concentration-dependent manner with no change in current kinetics (fig. 1B). It should be noted that F1579A shows both activation and fast inactivation but establishes a non-inactivating current apparent at end pulse not present in the WT-β_1, as previously described.[14] Figure

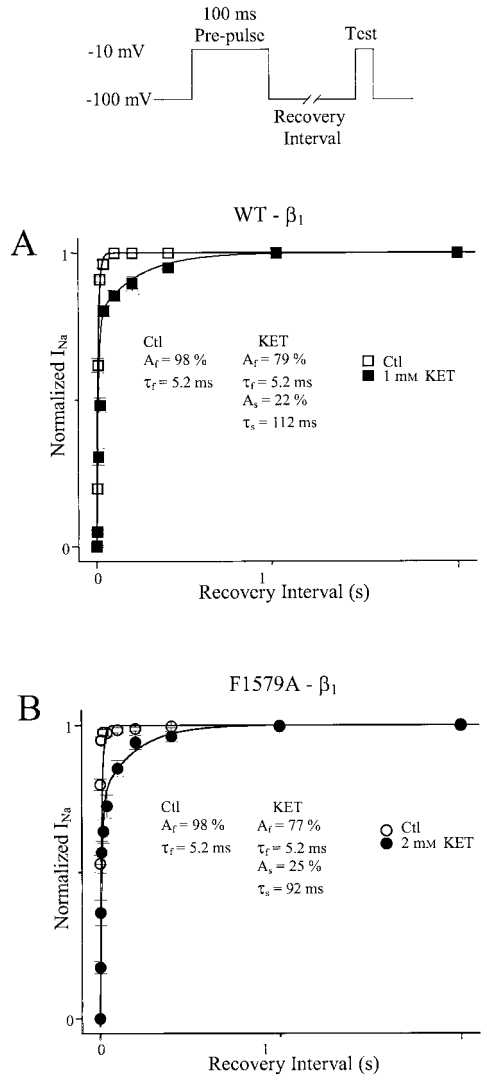

Fig. 3. Effects on recovery from depolarization-induced inactivation. The top panel displays the two-pulse protocol with varying recovery time intervals used. (*A*) Current amplitudes triggered by the test pulse normalized to the prepulse current value as a function of recovery interval. Without (open) and with (closed) 1 mM ketamine in WT-β_1 (n = 6). Solid lines are the monoexponential (for control) or biexponential (for with ketamine) fits to the recovery curves. (*B*) Same as for *A* except for F1579A-β_1 without (open) or with (closed) 2 mM ketamine (n = 7).

1C summarizes the concentration–response relation for normalized peak current for both WT-β_1 (concentration for half-maximal inhibition [IC_{50}] = 0.8 mM) and F1579A-β_1 (IC_{50} = 2.1 mM). Figure 1 reports the fraction of available unblocked resting channels as a function of ketamine concentration. The F1579A-β_1 mutation caused a more than twofold shift to the right without affecting the slope. This attenuated sensitivity to resting ketamine blockade implicates the intrapore receptor in the underlying mechanism. When the concentration–response curve was replotted after normalization for the shift in IC_{50}, no difference in ketamine blockade of WT-β_1 and F1579A-β_1 was seen (fig. 1D). The effect of the mutation appears to be a simple shift in the channel sensitivity to ketamine blockade.

We next tested for use-dependent inhibition using a pulse train protocol. Figure 2A plots superimposed I_{Na} elicited by the 1st and the 15th depolarizing steps. In control WT-β_1 (fig. 2A) and F1579A-β_1 with no ketamine (data not shown), there was little or no decrease in amplitude from the start to the end of the pulse train, indicating little accumulation of fast-inactivated channels. Approximately equipotent concentrations of ketamine, as determined from data shown in figure 1, were added to block WT-β_1 (1 mM) (fig. 2A) and F1579A-β_1 (2 mM). A use-dependent decrease in the current magnitude can be observed. Ketamine induced a progressive reduction of I_{Na} for WT-β_1, which reached an apparent plateau at the 9th pulse (fig. 2B). This reduction represents decreased channel availability resulting from accumulation of slowly recovering, depolarization-induced blockade caused by ketamine. The plateau is the point of equilibrium between intrapulse blockade and interpulse recovery and thus reports the steady-state fraction of available unblocked channels during a train of depolarizing pulses. For WT-β_1 this fraction was approximately 0.7. This contrasts with the 0.3 fraction reported for lidocaine phasic block of WT-β_1.[15] Although ketamine is more potent than lidocaine in tonic blockade (IC_{50} = 1.9 mM),[15] it is less potent in phasic blockade. As ketamine concentration increased, the steady-state phasic blockade (estimated by the current magnitude ratio between the 15th and the 1st pulse) increased (fig. 2C). The IC_{50} for phasic blockade of WT-β_1 was 2.3 mM. In F1579A-β_1, ketamine caused a similar concentration-dependent phasic blockade but shifted to the right compared with the WT-β_1 (fig. 2C). When replotted on a relative concentration axis, normalized by the IC_{50} for phasic blockade, functions relating ketamine concentration and phasic blockade were identical for WT-β_1 and F1579A-β_1 (fig. 2C). The mutation reduced ketamine sensitivity of the phasic blockade as well.

Recovery of Na^+ channels from depolarization-induced nonconducting states can be examined by a two-pulse protocol. Figure 3 plots normalized peak I_{Na} as a function of recovery time in the absence and presence of ketamine. In the absence of ketamine, both WT-β_1 and F1579A-β_1 recovery time courses were well described by a monoexponential function (τ_f = 5.2 ms), reflecting rapid recovery from the inactivated state. Ketamine introduced a second, slower component to the recovery time course for both WT-β_1 (τ_s = 112 ms) and F1579A-β_1 (τ_s = 92 ms). This slower component probably reflects recovery from a long-lived, drug-induced nonconducting state (see Vendantham and Cannon[16] and Chen *et al.*[17] for an alternative interpretation). The magnitudes of the slow components (22% for WT-β_1 and 25% for F1579A-β_1) were similar with equipotent concentrations of ketamine. This was not surprising in view of the finding

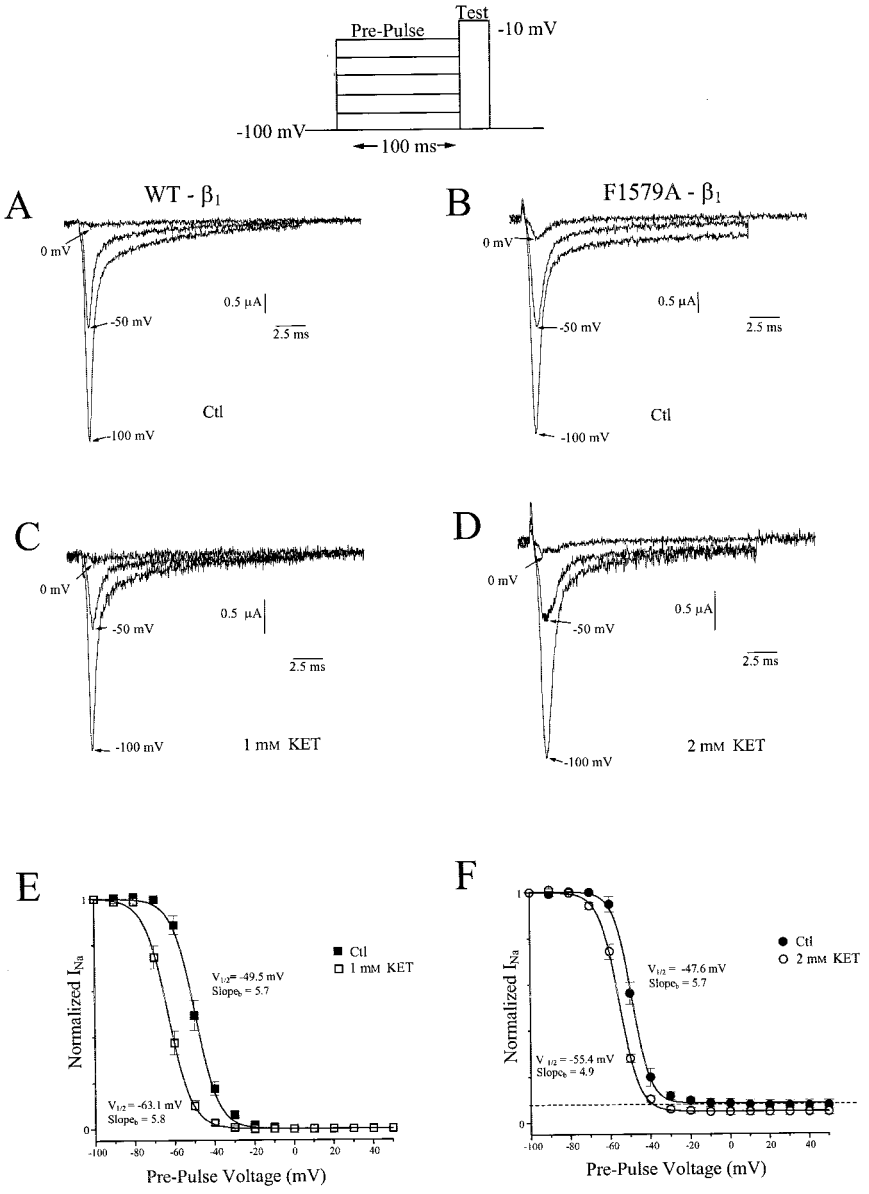

Fig. 4. A shift in the steady-state inactivation toward negative voltage. A two-pulse voltage protocol (*top*) was used to determine the voltage dependence of steady-state inactivation for WT-β_1 and F1579A-β_1. (*A–D*) Representative current traces elicited by the test pulse following the indicated prepulse voltages in control (Ctl) and ketamine (KET). (*E*) A plot of test Na^+ current (I_{Na}) normalized to control I_{Na} amplitude (test pulse with no prepulse) *versus* prepulse voltage without (solid) and with (open) 1 mM ketamine for WT-β_1. Smooth curves are Boltzmann function fits to the data with the indicated parameters. (*F*) Same as above (*E*) but for F1579A-β_1 and 2 mM ketamine. The dashed line indicates the fraction of channels not inactivated even at large depolarized prepulse voltages. For both summary figures, n = 5.

from the tonic and phasic blockade experiments (figs. 1 and 2) that the only effect of the point mutation was to decrease sensitivity to ketamine.

Local anesthetics also cause a hyperpolarizing shift in the steady-state inactivation curve of sodium channels. We employed a two-pulse protocol (fig. 4) to determine the effects of ketamine on the steady-state inactivation curve. To ensure an equilibrium between resting and fast-inactivated channels, we used a 100-ms prepulse. Figures 4A–D are current traces of I_{Na} for the WT-β_1 and F1579A-β_1 channels with and without ketamine. A prepulse voltage-dependent reduction in the current magnitude can be seen. Figures 4E and F plot normalized test I_{NA} as a function of prepulse voltage and display the voltage dependence of available channels. Without ketamine, for prepulse voltages less than −60 mV, all channels are available for opening during the test pulse. Increasing prepulse voltage reduces the fraction of available channels to zero near −20 mV; unavailable channels were presumably inactivated during the 100-ms prepulse. Fit of the data to the Boltzmann distribution demonstrated a half-activation voltage ($V_{½}$) of −63.1 mV with a slope of 5.8 for WT-β_1. Ketamine at 1 mM shifted the steady-state inactivation curve to the left decreasing $V_{½}$ to −49.5 mV (a 13.6-mV shift toward the negative potential) with no change in the slope, similar to the effect of other local anesthetics. In the same procedure, F1579A-β_1 showed a control $V_{½}$ of −55.4 mV and a plateau inactivation value of 0.1 even at large depolarizing prepulse voltages. Thus, the point mutation created a population of non-inactivated channels available even at depolarized prepulse potentials. After equipotent ketamine at 2 mM the F1579A-β_1 $V_{½}$ shifted negatively by 7.8 mV. Ketamine probably causes reduction of channel

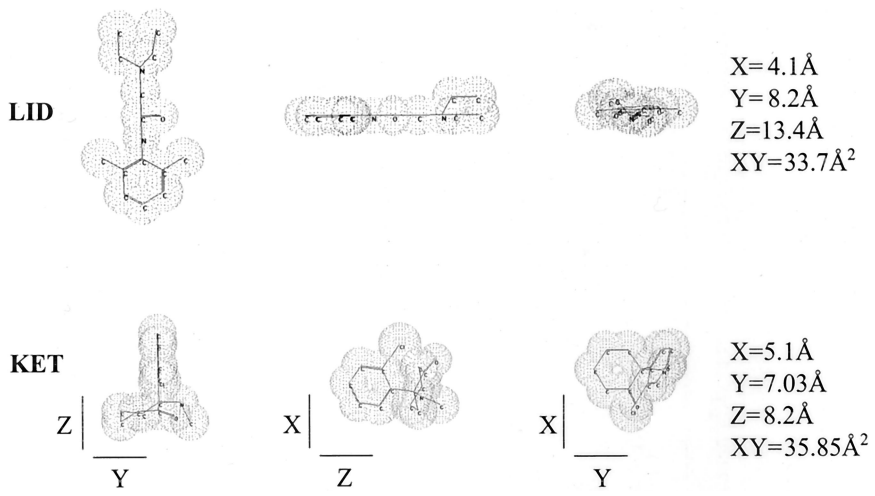

Fig. 5. Three-dimensional molecular modeling of ketamine (KET) and lidocaine (LID). Structures for the drugs were modeled using HyperChem (see Materials and Methods). The energetically optimized molecular conformation in an aqueous environment was rotated in space to align the two molecules along the indicated axes. For visual clarity, hydrogen atoms are not shown. Bars = 3.4 Å.

availability by stabilizing inactivated states. Its effect on $V_{½}$ shift is comparable to that of lidocaine. As was previously reported for etidocaine block of the rat brain sodium channel F1764A mutant,[11] the ketamine-induced $V_{½}$ shift was attenuated by the homologous skeletal muscle sodium channel F1579A mutant, albeit not as profoundly.

Discussion

Local Anesthetic–like Action of Ketamine

In the current study, we characterized the molecular pharmacologic effects of ketamine using recombinant voltage-gated sodium channels. We showed that ketamine blocks sodium channels in a local anesthetic–like fashion, including tonic blockade, phasic blockade, shift of the steady-state inactivation curve to the right, and a dependence of these actions on the intrapore local anesthetic site. These are hallmark features of local anesthetics.[8] We previously reported the effects of lidocaine on the same sodium channel clone[15]; many of the effects are reconfirmed in our present study (data not shown). Quantitative comparison between the effects of ketamine and the effects of lidocaine we previously reported revealed significant differences.[15] Ketamine is a more potent tonic blocker but a less potent use-dependent blocker. The greatest difference between the two drugs was in the time course of recovery from inactivation. In WT-β_1, lidocaine introduced a slow component to the recovery time course with a time constant of 490 ms. Ketamine-blocked channels also demonstrated a slowing of recovery from inactivation but with a recovery time constant of only 112 ms. Etidocaine, like lidocaine, introduced a much slower component (τ_s = 2,400 ms), and this effect was greatly attenuated in the intrapore local anesthetic site mutant.[11] Notably, a homologous site mutant in our skeletal muscle channel had no effect on the ketamine-induced slowing of recovery from inactivation (fig. 3). Ketamine appears less effective in stabilizing the inactivated state relative to lidocaine or etidocaine. The difference in the intrapore receptor site dependence of ketamine action suggests that the mechanism by which ketamine modulates inactivated channels may be fundamentally different from classic local anesthetics.

Structural Basis for Quantitative Differences between Ketamine and Lidocaine

Typically, local anesthetics such as lidocaine are tertiary amine molecules with a charged amine head and a lipophilic aromatic tail. There is evidence to suggest that this aromatic tail interacts with the intrapore local anesthetic receptor in the IVS6 by binding to the lipophilic pocket formed in part by residue F1579[18] or through π electron interactions between the two aromatic rings.[11,19] Structure-activity study of lidocaine-derivative binding to cardiac myocytes indicated an optimum arylamide-to-amine domain linker length of two carbons and an amine domain carbon length of four or more carbons.[20] Decreasing drug affinity for the receptor with increasing amino carbon length, regardless of the precise carbon arrangement, suggested that the amino-terminal "dissolves" in a hydrophobic pocket; the molecule does not have the classic "lock-and-key" receptor-ligand interaction. Ketamine's structure is quite different from the prototypical local anesthetic. It is not an amino ester or an amino amide. Ketamine does have a halide substituted aromatic tail, but the amine group is secondary rather than tertiary and is attached to a second carbon ring. However, if drug-receptor interaction is based on a hydrophobic interaction at both the aromatic and the amino ends of the molecule as suggested by Sheldon,[20] the structure of ketamine suggests that this molecule should act at the local anesthetic receptor site.

Generally, lipophilic local anesthetics such as benzocaine exhibit little use-dependent blockade of voltage-gated sodium channels because of a second hydrophobic pathway for drug escape from the channel pore.[9] This

results in the drug's inability to persistently stabilize the inactivated state. Courtney,[13] through three-dimensional molecular modeling of several local anesthetic–like molecules, arrived at a critical maximum dimension of 5 × 10 Å (or 50 Å^2) cross-sectional area for a molecule to access this hydrophobic pathway. The smallest cross-sectional area of ketamine (35.9 Å^2) (fig. 5) is similar to tocainide (36.6 Å^2) and much less than the access-limiting dimension of 50 Å^2. Therefore, the poor phasic blockade exhibited by ketamine is probably due to a rapid escape of this highly lipophilic molecule *via* the hydrophobic pathway.[21] However, the longevity of the ketamine blocked state (~100 ms) (fig. 3) is longer compared with benzocaine (< 50 ms), which exhibits no phasic blockade.[22]

The F1579A mutation lowered the affinity of ketamine for the ion channel, consistent with the prior suggestion that this mutation destabilizes the inactivated state, thereby reducing the apparent affinity of drugs acting on the inactivated state.[11,14] The F1579A mutant also reduced the ketamine-induced leftward shift of the steady-state inactivation curve, consistent with prior reports. However, there were differences in the effect of this mutation on ketamine interaction with the channel. F1579A did little to alter use-dependent inhibition or recovery from depolarization-induced blockade by ketamine. The same mutation greatly reduces lidocaine phasic blockade,[15] and a homologous mutation in different sodium channel isoforms essentially eliminates etidocaine[11] or tetracaine[23] phasic blockade. Likewise, etidocaine-induced slow recovery from inactivation is essentially eliminated by this point mutation.[11] This discrepancy between the effects of the mutation on ketamine and on two prototypic local anesthetics could be due to multiple structural determinants. Single-channel studies suggest two modes of lidocaine blockade, rapid and discrete, and that F1579 is a portion of the long-lived discrete binding pocket.[18,24] Ketamine, whose spatial topology is clearly different from lidocaine, may exhibit different affinity for the discrete and the rapid block sites, resulting in different consequences of the F1579A mutation. Interaction of a larger alkaloid molecule such as batrachotoxin with the sodium channel depends both on the IVS6 intrapore site mutated in our study, as well as on a distinct site on IS6.[25] Whether this remote site effects ketamine action is not known. Further structural and pharmacologic studies are required for a deeper understanding of these pore interactions.

Possible Use of Ketamine for Neuraxial Block?

Compared with lidocaine, the greater local anesthetic potency demonstrated in the current study and less neurotoxicity exhibited by ketamine[26–28] suggest the potential utility of ketamine as an intrathecal local anesthetic. In addition, the well-known *N*-methyl-D-aspartate (NMDA) receptor antagonist property of ketamine might prevent central sensitization and the development of neuropathic pain[29–31] and might even reduce the development of opioid tolerance.[32–34] However, clinical experience suggests that the central side effects limit the utility of low doses of ketamine as a single agent or even as an adjuvant for neuraxial block.[5–7] At the present time, ketamine, despite exhibiting local anesthetic–like properties, seems not to be a suitable agent for subarachnoid block in humans. If the molecular underpinning responsible for the sodium channel block can be separated from the nonspecific NMDA antagonist property and the resultant central side effects, chemical alterations of ketamine could result in an ideal molecule with minimal toxicity and potent inhibition of the sodium channel. Such a compound would be an ideal agent for use in subarachnoid regional anesthesia.

The authors thank Jennifer Wagner (The Verdi Group, Rochester, NY) for her assistance with the illustrations.

References

1. Zhou ZS, Zhao ZQ: Ketamine blockage of both tetrodotoxin (TTX)-sensitive and TTX-resistant sodium channels of rat dorsal root ganglion neurons. Brain Res Bull 2000; 52:427–33
2. Hara Y, Chugun A, Nakaya H, Konda H: Tonic block of the sodium and calcium currents by ketamine in isolated guinea pig ventricular myocytes. J Vet Med Sci 1998; 60:479–83
3. Benoit E: Effects of intravenous anaesthetics on nerve axons. Eur J Anaesthesiol 1995; 12:59–70
4. Gomez de Segura IA, De Rossi R, Santos M, Lopez San-Roman J, Tendillo FJ, San-Roman F: Epidural injection of ketamine for perineal analgesia in the horse. Vet Surg 1998; 27:384–91
5. Bion JF: Intrathecal ketamine for war surgery: A preliminary study under field conditions. Anaesthesia 1984; 39:1023–8
6. Hawksworth C, Serpell M: Intrathecal anesthesia with ketamine. Reg Anesth Pain Med 1998; 23:283–8
7. Kathirvel S, Sadhasivam S, Saxena A, Kannan TR, Ganjoo P: Effects of intrathecal ketamine added to bupivacaine for spinal anaesthesia. Anaesthesia 2000; 55: 899–904
8. Catterall WA, Mackie K: Local anesthetics, The Pharmacological Basis of Therapeutics, 9th edition. Edited by Hardman JG, Limbird LE. New York, McGraw-Hill, 1996, pp 331–47
9. Hille B: Mechanisms of block, Ionic Channels of Excitable Membranes, 2nd edition. Sunderland, MA, Sinauer Associates, 1992, pp 390–422
10. Frenkel C, Urban BW: Molecular actions of racemic ketamine on human CNS sodium channels. Br J Anaesth 1992; 69:292–7
11. Ragsdale DS, McPhee JC, Scheuer T, Catterall WA: Molecular determinants of state-dependent block of Na+ channels by local anesthetics. Science 1994; 265: 1724–28
12. Howard A, McIver J, Collins J: Using molecular mechanics, Computational Chemistry, Waterloo, Ontario, Canada, HyperChem, 1994, pp 83–8
13. Courtney KR: Why do some drugs preferentially block open sodium channels? J Mol Cell Cardiol 1988; 20:461–4
14. McPhee JC, Ragsdale DS, Scheuer T, Catterall WA: A critical role for transmembrane segment IVS6 of the sodium channel α subunit in fast inactivation. J Biol Chem 1995; 270:12025–34
15. Wagner II LE, Eaton M, Sabnis SS, Gingrich KJ: Meperidine and lidocaine block of recombinant voltage-dependent Na^+ channels: Evidence that meperidine is a local anesthetic. ANESTHESIOLOGY 1999; 91:1481–90
16. Vendantham V, Cannon SC: The position of the fast-inactivation gate during lidocaine block of voltage gated Na^+ channels. J Gen Physiol 1999; 113:7–16
17. Chen Z, Ong BH, Kambouris NG, Marban E, Tomaselli GF, Balser JR: Lidocaine induces a slow inactivated state in rat skeletal muscle sodium channels. J Physiol (Lond) 2000; 524:37–49
18. Kimbrough JT, Gingrich KJ: Quaternary ammonium block of mutant Na^+ channels lacking inactivation: Features of a transition-intermediate mechanism. J Physiol (Lond) 2000; 529:93–106
19. Wright SN, Wang SY, Kallen RG, Wang GK: Differences in steady-state inactivation between Na channel isoforms affect local anesthetic binding affinity. Biophys J 1997; 73:779–88

20. Sheldon RS, Hill RJ, Taquis M, Wilson LM: Aminoalkyl structural requirements for interaction of lidocaine with the class I antiarrythmic drug receptor on rat cardiac myoctyes. Mol Pharmacol 1991; 39:69–14

21. Hille, B: Local anesthetics: Hydrophilic and hydrophobic pathways for the drug-receptor reaction. J Gen Physiol 1997; 69:497–515

22. Wang GK, Qual C, Wang SY: A common local anesthetic receptor for benzocaine and etidocaine in voltage-gated $\mu 1$ Na^+ channels. Pflugers Arch 1998; 435:293–302

23. Li HL, Galue A, Meadows L, Ragsdale DS: A molecular basis for the different local anesthetic affinities of resting versus open and inactivated states of the sodium channel. Mol Pharmacol 1999; 55:134–41

24. Gingrich K, Beardsley D, Yue DT: Ultra-deep blockade of Na^+ channels by a quaternary ammonium ion: Catalysis by a transition-intermediate state? J Physiol (Lond) 1993; 471:319–41

25. Linford NJ, Cantrell AR, Qu Y, Scheuer T, Catterall WA: Interaction of batrachotoxin with the local anesthetic receptor site in the transmembrane segment IVS6 of the voltage-gated sodium channel. Proc Natl Acad Sci U S A 1998; 95:13947–52

26. Borgbjerg FM, Svensson BA, Frigast C, Gordh T: Histopathology after repeated intrathecal injections of preservative-free ketamine in the rabbit: A light and electron microscopic examination. Anesth Analg 1994; 79:105–111

27. Stotz M. Oehen HP, Gerber H: Histological findings after long-term infusion of intrathecal ketamine for chronic pain: A case report. J Pain Symptom Manage 1999; 18:223–8

28. Karpinski N, Dunn J, Hansen L, Masliah E: Subpial vacuolar myelopathy after intrathecal ketamine: Report of a case. Pain 1997; 73:103–5

29. Woolf CJ, Mannion RJ: Neuropathic pain: Aetiology, symptoms, mechanisms, and management. Lancet 1999; 353:1959–64

30. Burton AW, Lee DH, Saab C, Chung JM: Preemptive intrathecal ketamine injection produces a long-lasting decrease in neuropathic pain behaviors in a rat model. Reg Anesth Pain Med 1999; 24:208–13

31. Takahashi H, Miyazaki M, Nanbu T, Yanagida H, Morita S: The NMDA-receptor antagonist ketamine abolishes neuropathic pain after epidural administration in a clinical case. Pain 1998; 75:391–4

32. Joo G, Horvath G, Klimscha W, Kekesi G, Dobos I, Szikszay M, Benedek G: The effects of ketamine and its enantiomers on the morphine- or dexmedetomidine-induced antinociception after intrathecal administration in rats. ANESTHESIOLOGY 2000; 93:231–41

33. Miyamoto H, Saito Y, Kirihara Y, Hara K, Sakura S, Kosaka Y: Spinal coadministration of ketamine reduces the development of tolerance to visceral as well as somatic antinociception during spinal morphine infusion. Anesth Analg 2000; 90:136–41

34. Simoyama N, Simoyama M, Inturrisi CE, Elliott KJ: Ketamine attenuates and reverses morphine tolerance in rodents. ANESTHESIOLOGY 1996; 85:1357–66